Journal of Experimental Marine Biology and Ecology 595 (2026) 152169

Contents lists available at ScienceDirect

Journal of Experimental Marine Biology and Ecology

journal homepage: www.elsevier.com/locate/jembe

Ecological impact of macroalgae secondary metabolites on fatty acid and amino acid profiles of *A. lixula* sea urchin in the Mediterranean Sea

Manuela Mauro [a,1], Rosario Badalamenti [a,1], Giovanna Cafeo [b], Valentina Chiaia [b], Danilo Donnarumma [b], Mirella Vazzana [a,c], Vincenzo Arizza [a,c], Giuseppe Micalizzi [b,*], Paola Dugo [b,d], Luigi Mondello [b,d], Francesca Falco [e]

[a] *Department of Biological, Chemical and Pharmaceutical Sciences and Technologies (STEBICEF), University of Palermo, Via Archirafi 18, 90123 Palermo, Italy*
[b] *Messina Institute of Technology c/o Department of Chemical, Biological, Pharmaceutical and Environmental Sciences, University of Messina, Viale G. Palatucci 13, 98168 Messina, Italy*
[c] *NBFC, National Biodiversity Future Center, Piazza Marina 61, 90133 Palermo, Italy*
[d] *Chromaleont s.r.l., c/o Department of Chemical, Biological, Pharmaceutical and Environmental Sciences, University of Messina, Viale G. Palatucci 13, 98168 Messina, Italy*
[e] *Institute for Biological Resources and Marine Biotechnologies (IRBIM- CNR), via L Vaccara, 61. 91026 Mazara del Vallo, Italy*

ARTICLE INFO

Keywords:
Ecotoxicology
Invasive species
Sea urchin
Macroalgae
FAMEs GC analysis
OPA amino acids HPLC-FLD analysis

ABSTRACT

The introduction of non-native species into marine ecosystems can alter trophic interactions and influence the physiology of native organisms. Understanding these biochemical interactions is essential to assess the ecological impact of these species on local biodiversity. For the first time, the following study evaluates the effects of different macroalgae secondary metabolites on fatty acid and amino acid profiles of sea urchin *Arbacia lixula* (Linnaeus, 1758) from the Mediterranean Sea. The macroalgae involved in this study were *Ericaria brachycarpa*, an endemic species of the Mediterranean, and *Asparagopsis taxiformis*, an allochthonous invasive species. Gas chromatography-mass spectrometry (GC–MS) and gas chromatography-flame ionization detection (GC-FID) techniques were employed for the elucidation of the fatty acids, while amino acids were investigated by means of high-performance liquid chromatography coupled to fluorescence detector (HPLC-FLD). The impact of macroalgae metabolites on the fatty acids and amino acids in *A. lixula* species was evaluated after exposures at 24 and 48 h. Analytical results revealed that *E. brachycarpa* and *A. taxiformis* metabolites determined a significant change in levels of fatty acids (PUFAs, MUFAs, and SFAs) compared to untreated *A. lixula* species in accordance with their susceptibility to oxidation mechanisms. Also, macroalgae secondary metabolites induced distinct and time dependent metabolic reprogramming in *A. lixula* uncovering a biphasic oxidative stress response, membrane remodeling, and amino acids compensation mechanisms.

1. Introduction

Macroalgae are sessile organisms that have chemical strategies to cope with the environmental and biological pressures of marine habitats. Among these strategies, the production of secondary metabolites represents a key defensive mechanism against herbivory, interspecific competition, and biotic stressors. These compounds include sterols, terpenes, polyphenols, and low-molecular-weight halogenated molecules, which contribute to the chemical specificity and marked interspecific diversity of macroalgae (Maschek and Baker, 2008; Paul and Pohnert, 2011). Several studies have shown that algal secondary metabolites can exert immunomodulatory, antimicrobial, antioxidant, and cytotoxic effects on exposed marine organisms, thereby significantly influencing their physiological processes and metabolic regulation (Mishra, 2018; Nunes et al., 2018; Shalaby and Shanab, 2021; Thépot et al., 2022). In particular, algal species are also known for their ability to produce numerous halogenated compounds (McConnell and Fenical, 1977), including polyhalomethanes (such as $CHCl_3$ or CH_2Br_2), catalyzed by haloperoxidases (HPO) (Butler and Carter-Franklin, 2004; Butler and Sandy, 2009; Neumann et al., 2008). These highly reactive

* Corresponding author.
E-mail address: giumicalizzi@unime.it (Giuseppe Micalizzi).
[1] These authors contributed equally.

https://doi.org/10.1016/j.jembe.2026.152169
Received 12 October 2025; Received in revised form 28 January 2026; Accepted 29 January 2026
Available online 3 February 2026

metabolites are of special ecological relevance, as they can act as potent chemical stressors for surrounding organisms and play a central role in mediating algal–herbivore interactions.

In the Mediterranean Sea, habitat-forming brown macroalgae of the *Cystoseira sensu lato* complex form structurally complex algal forests that play a pivotal ecological role by providing habitat complexity, nursery grounds, and trophic resources for a wide range of marine organisms (Ballesteros et al., 2009; Cheminée et al., 2013). *Ericaria brachicarpa* (synonyms *Cystoseira brachycarpa* and *Carpodesmia brachycarpa*) is an endemic Mediterranean species that contributes to the formation of structurally complex algal forests, which are widely recognized as indicators of high ecological status in coastal waters according to the European Water Framework Directive (Directive 2000/60/EC, 2000). These assemblages support high biodiversity and promote ecosystem stability by buffering physical stress and regulating community structure (Ballesteros et al., 2009). Regarding species of the *Cystoseira sensu lato* complex, the main compounds produced include fucoidans, polyphenols, photosynthetic pigments, alginates and terpenes (El-Beltagi et al., 2022; El-Sheekh et al., 2022; Matos et al., 2021). Numerous molecules have been identified in different species of the *Ericaria* genus, including terpenoids, steroids, phlorotannin and phenolic compounds, some with antimicrobial and anticancer properties (Amico et al., 1981).

Asparagopsis taxiformis genus, belonging to the Bonnemaisoniales order of the Rhodophyta phylum, was recently grouped among the 100 worst invasive macroalgae species (Mancuso et al., 2022). Its rapid spread and competitive success have been associated with both physical habitat alteration and the release of highly bioactive secondary metabolites (Ponte et al., 2022). In recent decades, *A. taxiformis* has been registered in several Mediterranean countries, particularly in Spain (Ballesteros and Rodríguez-Prieto, 1996), Italy (Barone et al., 2003) and Greece (Tsiamis and Panayotidis, 2007). Negative effects on native marine communities have been associated with *A. taxiformis* species. However, much of its ecological impact is still poorly understood (Zanolla et al., 2018).

In the Mediterranean Sea, sea urchins are the main consumers of macroalgae such as species belonging to the *Cystoseira sensu lato* complex (Agnetta et al., 2015; Piazzi and Ceccherelli, 2019). In particular, *Arbacia lixula,* belonging to the class Echinoidea, is widespread in the Mediterranean Sea and the eastern Atlantic. *Arbacia lixula* is a common and ecologically relevant species in shallow rocky habitats, where it can reach high population densities and exert strong grazing pressure. Through its scraping activity mediated by the Aristotle's lantern, *A. lixula* plays a primary role in regulating the composition and abundance of macroalgal assemblages and is a key driver of the transition from algal forests to barren grounds under high-density conditions (Bonaviri et al., 2011; Privitera et al., 2008). Beyond physical grazing, macroalgal–sea urchin interactions are also mediated by chemical mechanisms, as secondary metabolites produced by macroalgae act as chemical defenses against herbivory and competition (Budzałek et al., 2021; Hay, 2009). These compounds can directly affect the physiology of primary consumers, inducing sublethal physiological responses in sea urchins by altering key metabolic pathways involved in oxidative stress regulation, membrane integrity, and energy balance (Quetglas-Llabrés et al., 2020; Tejada et al., 2013). In this context, fatty acids and amino acids represent particularly informative metabolic endpoints, as fatty acids are central to membrane structure and susceptibility to lipid peroxidation, while amino acids play key roles in energy metabolism, redox homeostasis, and stress compensation mechanisms.

Accordingly, *A. lixula* represents an ecologically relevant model organism to investigate metabolically mediated physiological responses to algal chemical stress, providing mechanistic insight into algae–herbivore interactions beyond physical grazing alone.

The impact of macroalgae secondary metabolites on the metabolic pathways involving fatty acids and amino acids in primary consumers like *A. lixula* remain poorly understood despite the recognized ecological importance of chemical- mediated algae-herbivore interactions. In this context, high concentration levels of bioactive lipophilic substances from *A. taxiformis* have attracted more scientific attention. Neethu et al. (2017) showed that chloroform *A. taxiformis* extracts had the best antioxidant activity and the highest total flavonoid content than other extracts obtained using different solvents. These characteristics indicate a possible effect on exposed marine creature's lipid metabolism. Similarly, chloroform *Cystoseira brachycarpa* extracts revealed a chemical profile rich in diterpenes, bioactive compounds known for their ability to modulate oxidative stress and redox processes (Amico et al., 1981).

However, a direct comparative assessment of the metabolic effects induced by secondary metabolites from native *versus* invasive macroalgae on a key Mediterranean herbivore is still lacking. The present study aims to investigate the effects of secondary metabolites from the native macroalga *Ericaria brachycarpa* and the invasive *Asparagopsis taxiformis* on fatty acid and amino acid metabolism in the sea urchin *Arbacia lixula*. We hypothesized that direct exposure to secondary metabolites from chemically contrasting macroalgae would elicit distinct sublethal metabolic responses in *A. lixula*. Specifically, we expected that metabolites from *A. taxiformis*, characterized by a highly reactive and halogenated chemical profile, would induce a stronger and more rapid modulation of fatty acid and amino acid metabolic pathways associated with oxidative stress regulation, membrane integrity, and energy balance compared to those from *E. brachycarpa*.

2. Materials and methods

2.1. Chemicals

2.1.1. Solvents and reagents

Chloroform ($CHCl_3$, for HPLC), methanol (MeOH, for HPLC), *n*-heptane (suitable for HPLC), water (LC-MS grade) and tetrahydrofuran (THF, for HPLC) solvents were purchased by Merck Life Science (Merck KGaA, Darmstadt, Germany). Boron trifluoride-methanol solution (BF_3, 14% in methanol), and sodium methoxide solution (MeONa, 0.5 M for GC derivatization) were acquired from Merck Life Science. Hydrochloric acid (HCl, 4 N and 36%), sodium acetate, *orto*-phthaldialdehyde (OPA), sodium borate, 2-mercaptoethanol, and Tween 80 (viscous liquid) reagents were acquired from Merck Life Science.

Seawater was prepared using Instant Ocean Sea Salt (Mentor, OH, USA) dissolved in deionized water corrected for salinity (38–39‰) and pH (8.1 ± 0.1). Dimethyl sulfoxide (DMSO, ≥99.9% purity), was purchased from Sigma-Aldrich (St. Louis, MO, USA) and artificial coelomic fluid, ACF (10 mM $CaCl_2$; 14 mM KCl; 50 mM $MgCl_2$; 398 mM NaCl; 1.7 mM Na_2HCO_3; 25 mM Na_2SO_4) was prepared as suggested by Terwilliger et al. (2007).

2.1.2. Analytical standards

A certified mix of amino acid standards (2.5 μmoles per mL in 0.1 N HCl, Merck Life Science) containing L-Alanine (Ala), L-Arginine (Arg), L-Aspartic acid (Asp), L-Cystine (Cys), L-Glutamic acid (Glu), Glycine (Gly), L-Histidine (His), L-Isoleucine (Ile), L-Leucine (Leu), L-Lysine (Lys), L-Methionine (Met), L-Phenylalanine (Phe), L-Proline (Pro), L-Serine (Ser), L-Threonine (Thr), L-Tyrosine (Tyr), and L-Valine (Val) was used for HPLC-FLD method development. Analytical standard α-aminobutyric acid (Aba), used as internal standard (ISTD), was purchased from Merck Life Science. A homolog series of carbon saturated FAMEs (C_4-C_{24}, Merck Life Science) was used for calculating linear retention index (LRI) values in GC–MS analysis.

2.2. Sampling

Twenty-four specimens of the sea urchin *A. lixula* were collected from the waters of Palermo, along the north coast of Sicily, at a depth of 5–10 m and lying near a *Posidonia oceanica* seagrass meadow. The samples were maintained at a temperature of 15 °C thermostatically controlled, aerated in a 150 L glass aquarium with filtered seawater. A

small volume of water (10−20 L) was changed weekly, and the animals were fed once a week with commercial invertebrate food (Azoo, Taikong Corporation,Taipei, Taiwan).

2.3. Algae extract preparation

E. brachycarpa sporophytes and *A. taxiformis* gametophytes were collected in the Gulf of Palermo (Sferracavallo, Punta Barcarello). They were washed in order to remove debris and epiphytes, and then dried at 40 °C in an oven for 48 h. The dried thalli were then finely ground to obtain a powder. Secondary metabolite extracts from the *E. brachycarpa* and *A. taxiformis* macroalgae were performed by the Soxhlet extraction using $CHCl_3$ as the extraction solvent (Neethu et al., 2017). The extraction yields for *E. brachycarpa* and *A. taxiformis* were of 176 mg mL^{-1} and 118 mg mL^{-1}, respectively.

2.4. A. lixula treatment with macroalgae extracts

Sea urchins were treated with extracts of *E. brachycarpa* and *A. taxiformis* for 24 and 48 h. Injections were performed using artificial coelomic fluid (ACF) as vehicle, prepared according to Terwilliger et al. (2007). Algal extracts were evaporated to dryness to remove the solvent, and the dry residue was reconstituted in DMSO prior to administration. In the *E. brachycarpa* group (6 animals), each sea urchin was intracoelomically injected with 100 μL consisting of 7 μL of extract (88 mg mL^{-1} in DMSO; equivalent to 0.616 mg per individual) and 93 μL of ACF (final DMSO 7% *v/v*). In the *A. taxiformis* group (6 animals), each animal received 100 μL composed of 11 μL of extract (59 mg mL^{-1} in DMSO; equivalent to 0.649 mg per individual) and 89 μL of ACF (final DMSO 11% *v/v*). Control animals received 100 μL of vehicle (ACF + DMSO) adjusted to match the final DMSO concentration of the treatment groups (6 animals as controls for the 24 h group and 6 animals as controls for 48 h group). Coelomic fluid was collected from animals after 24 h and 48 h post-injection for the evaluation of treatment effects.

2.5. Coelomic fluid sampling

A. lixula coelomic fluids were collected using a sterile 5 mL syringe by gently piercing the peristomal membranes. The sampled fluids included both the cellular fraction (rich in coelomocytes) and the plasma fraction (Beijnink et al., 1984; Pereira et al., 2013), both known to be rich in proteins, lipids, and amino acids (Liyana-Pathirana et al., 2002). The coelomic fluid samples were transferred into sterile 15 mL tubes, immediately frozen, and stored at −80 °C until analysis. This procedure allowed for the preservation of sample integrity and the stability of metabolites for subsequent chemical analyses.

2.6. Fatty acids analysis

2.6.1. Lipid extraction

Total lipids of coelomic fluids were extracted by using Bligh & Dyer protocol (Bligh and Dyer, 1959), with some minor modifications. In detail, a volume of 7.5 mL of a $CHCl_3$/MeOH (1:2 *v/v*) solvent mixture was added to 2.5 mL of samples contained in a 50 mL-conical centrifuge tube; the mixture was homogenized using vortex mixer for 15 min. After, 2.5 mL of $CHCl_3$ and 2.5 mL of NaCl aqueous solution were added to the extraction mixture; the mixture was homogenized using vortex mixer and centrifuged (NEYA 16R centrifuge, NEYA ROTORS) at 3.000 rpm for 15 min. The lower chloroform phase containing lipid compounds was collected by using Pasteur pipette and transferred into an 8 mL amber vial. Lipids extract in chloroform was dried with an EZ-2 (EZ-2 Personal-Evaporator, Genevac) evaporator.

2.6.2. Lipid derivatization and GC analyses of FAMEs

FAs derivatization was carried out according to Micalizzi et al. (2024). In detail, 500 μL of MeONa methanolic solution were added to the lipid extract, sonication for 5 min, and heating for 30 min at 95 °C. After cooling, 500 μL of BF_3 methanolic solution were added to the reaction mixture; the solution was heated for 30 min at 95 °C. Finally, 300 μL of *n*-heptane and 200 μL of water solvent were added to the mixture. The upper layer containing the FAME derivatives was injected into the GC–MS and GC-FID systems for comprehensive FA profiling.

FAMEs GC–MS and GC-FID analyses were performed on the GCMS-QP2020 NX and Nexis GC-2030 (Shimadzu, Duisburg, Germany) systems, respectively. The gas chromatographs were equipped with an AOC-20i auto injector, a split/splitless injector (280 °C), and a straight FocusLiner™ design (wool packed) (Merck Life Science) of dimensions 95 mm × 5.0 mm OD × 3.4 mm ID (liner volume 810 μL). FAMEs GC separation was obtained by using a SLB-IL60i capillary column of 30 m × 0.25 mm ID × 0.20 μm d_f (Merck Life Science). The temperature program was as follows: 50 °C to 280 °C at 3.0 °C min^{-1}. Helium was used as carrier gas at a constant linear velocity of 30 cm s^{-1}, corresponding to an inlet pressure 31.7 kPa for GC–MS and 103.5 kPa for GC-FID. Volume injection was 2.0 μL (split ratio 1:10).

MS parameters were as follows: mass range 40–550 *m/z*; ion source temperature 220 °C; interface temperature 250 °C; software GCMS solution (Shimadzu, ver. 4.54). The FAMEs identity was established through MS similarity spectra (> 85%) and linear retention index (LRI) criteria. The identification of FAMEs was carried out by using a commercial mass spectral database, namely LIPIDS GC–MS Library (Chromaleont Srl, Messina, Italy).

FID parameters: temperature 280 °C; sampling rate 40 ms; hydrogen 40 mL min^{-1}; make-up gas (nitrogen) 10 mL min^{-1}; air 400 mL min^{-1}; software LabSolutions (Shimadzu, ver. 5.117). Each sample was injected into triplicate for a major data precision. Quantitative results were expressed in terms of percentage (%) area (peak area normalization). For better data precision, all the samples were analyzed in triplicates.

2.7. Total amino acids analysis

2.7.1. Hydrolysis of protein

A volume of 500 μL of coelomic fluid was added in a 4 mL glass vial with 50 μL of ISTD (Aba, 2.5 μmol mL^{-1}). The hydrolysis of samples was carried out by using 500 μL of hydrochloric acid (HCl, 36%). The glass vial was filled with nitrogen for one min and capped. Then, the vial was placed in an oven at 110 °C for 24 h. After the hydrolysis, the sample was dried carefully under flow of nitrogen gas. Finally, 500 μL of water was added to the vial and the solution was derivatized as reported below.

2.7.2. OPA-amino acids derivatization

OPA derivatizing solution was prepared by dissolving 50 mg of OPA reagent in 1.25 mL of MeOH, followed by addition of 11.2 mL of an aqueous solution of sodium borate 0.04 M (pH 9.5), 50 μL of 2-mercaptoethanol and 0.4 mL of Tween 80 (Dai et al., 2014). The online derivatization of AAs was carried out in automatic manner using a SIL-30 AC autosampler for Nexera-X2 system (Shimadzu) as follows: 50 μL of hydrolyzed sample and 50 μL of OPA solution were transferred into 2 mL autosampler vial fitted with 200 μL insert. The derivatization reaction was performed at room temperature (25 °C) for 7 min (stand-by). After, the OPA-AAs derivatives were automatically injected into the HPLC system for chromatographic separation and quantification.

2.7.3. Calibration and quantification of amino acids

A certified analytical balance (Shimadzu, Serie AP Mod. AP224W, d = 0.1 mg) was used to prepare a solution of Aba (ISTD) at a concentration of 2.5 μmol mL^{-1}. In detail, 25.0 mg of pure standard were weighted and solubilized in water into a 10 mL volumetric flask. The quantification of OPA-AAs was performed by using the calibration curve method. Calibration curves were constructed for OPA-AAs by diluting the certified mix of AA standards (2.5 μmol mL^{-1}) in water. Specifically, six concentration levels were constructed as follows: 500, 250, 100, 50, 25, and 10 nmol mL^{-1}. All calibration mixtures were spiked with a fixed

volume (50 μL) of the ISTD solution and subjected to the AAs derivatization procedure as previously described. After, the mixtures were analyzed by HPLC-FLD (four replicates for each calibration level). Finally, the linearity was measured by plotting the concentration ratio between target component and ISTD along the horizontal axis and the peak area ratio along the vertical axis. Limit of detection (LoD) and limit of quantification (LoQ) values were determined according to the Eurachem guidelines (Eurachem Guide, 2025). Specifically, the following formulas were applied: LoD = 3 × s'$_0$ and LoQ = 10 × s'$_0$, where s'$_0$ is the ratio between the standard deviation of the results expressed in concentration units and the square root of the number of replicates (n = 10).

2.7.4. OPA-amino acids HPLC-FLD analysis

HPLC-FLD analysis was performed on a Nexera-X2 system (Shimadzu), equipped with a RF-20AXS fluorescence detector. A previously developed method by Dai and co-workers (Dai et al., 2014) was used with slightly modification. The chromatographic separation was carried out on an Ascentis C18 column (150 cm × 4.6 mm, 2.7 μm) (Merck Life Science), kept at 25 °C. Mobile phase A was water/MeOH/THF (90.5:9.0:0.5 *v/v/v*) plus sodium acetate 0.1 M and 0.01% HCl (4 N); mobile phase B was MeOH. The gradient was as follows: 0 min, 14% B; 3 min, 14% B; 17 min, 20% B; 21 min, 30% B; 21.1 min, 45% B; 27 min, 50% B; 29 min, 70% B; 33 min, 100% B; 35 min, 100% B; 35.1 min, 14% B hold for 7 min. The injection volume was 5 μL. Peaks were recorded using 340 nm as excitation wavelength and 455 nm as emission wavelength. Data acquisition and processing were performed by LabSolution software (Shimadzu, ver. 5.85). All samples were analyzed in triplicate.

2.8. Statistical analysis of fatty acids and amino acids

All the statistical treatments were performed by using Excel 365 (Microsoft) for the evaluation of significant changes among the most abundant FAME and OPA-AA derivatives in untreated and treated coelomic fluid samples. Data scedasticity was evaluated by using a two tailed *F*-test ($p < 0.05$ were considered as heteroscedastic). Statistically significant differences were evaluated by using a two tailed *t*-test ($p < 0.05$ were considered statistically significant).

3. Results

3.1. Fatty acids profiling

The impact of *E. brachycarpa* and *A. taxiformis* extracts on the lipid metabolism of *A. lixula* coelomic fluids was investigated after 24 and 48 h of exposure. GC–MS analyses revealed the presence of thirty-two compounds belonging to different fatty acids classes such as saturated (SFAs), monounsaturated (MUFAs), and polyunsaturated (PUFAs) fatty acids. As an example, GC–MS chromatogram of FAMEs detected in coelomic fluid sample (control at 48 h) is reported in Fig. 1, while the samples treated with secondary metabolites from *A. taxiformis* and *E. brachycarpa* at 48 h were included in Fig. S1. Mass spectral similarity values and the correspondence between experimental and reference LRIs, useful for the peak identification, are reported in Table S1.

GC-FID analyses showed that the most abundant saturated compounds were the myristic (C14:0), palmitic (C16:0), and stearic (C18:0) acids, while the MUFAs class was mainly represented by the oleic acid (C18:1ω9) and by two isomers of the eicosenoic acid (C20:1ω12 and C20:1ω11). Finally, eicosadienoic (C20:2ω9), arachidonic (C20:4ω6), and eicosapentaenoic (C20:5ω3) acids were the most abundant components belonging to the PUFAs class. All these compounds accounted for more than 85% of the entire lipid fraction identified. Moreover, the FA profiles in the control samples of *A. lixula* showed a predominance of MUFAs and PUFAs, with EPA (C20:5ω3) levels around 11% and a significant proportion of eicosenoic acid isomers (C20:1ω11 and C20:1ω12). The relative abundances of the thirty-two FAMEs in the coelomic fluids of *A. lixula* control at 24 h and 48 h, and relative samples treated with *E. brachycarpa* and *A. taxiformis* extract algae are summarized in Table 1.

In order to evaluate the impact of secondary metabolites coming from the two algal species on the lipid profile of *A. lixula* coelomic fluid, a statistical treatment of the quantitative data, expressed in terms of

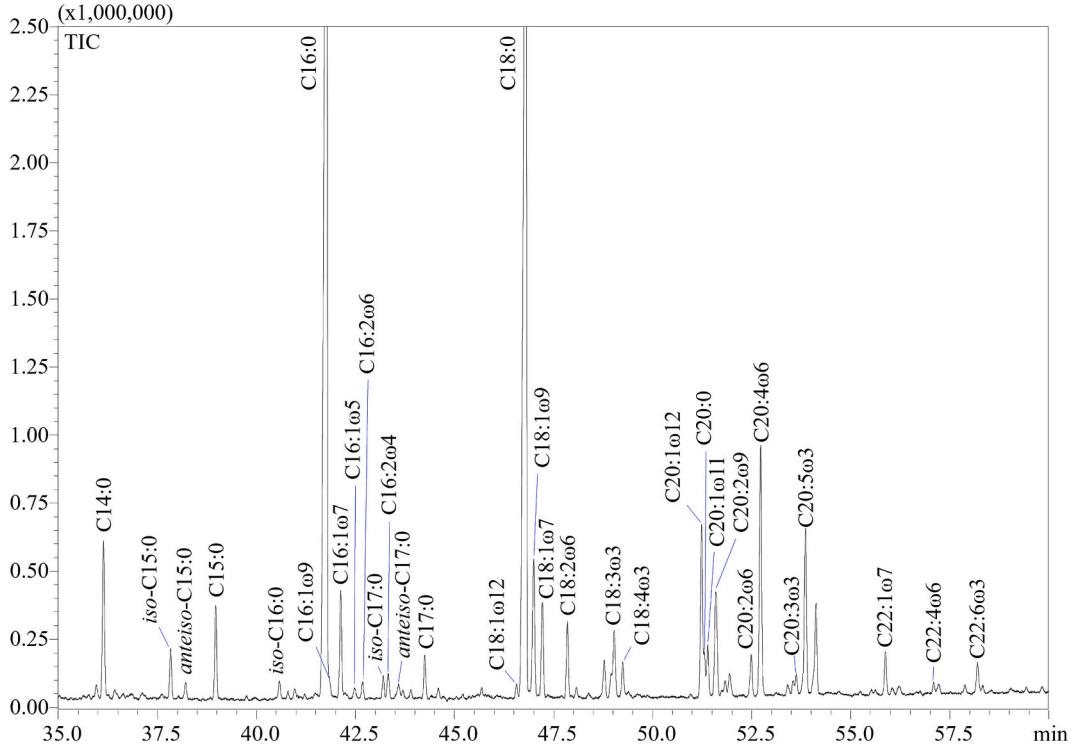

Fig. 1. GC–MS chromatogram of FAMEs in *Arbacia lixula* coelomic fluid (control sample at 48 h).

Table 1
FAMEs relative concentrations (mean % ± standard deviation) quantified in the coelomic fluids of *A. lixula* following 24 h and 48 h of exposure to extracts of *E. brachycarpa* and *A. taxiformis* algae as well as the respective controls (no treatment).

FAMEs	24 h			48 h		
	Control	*E. brachycarpa*	*A. taxiformis*	Control	*E. brachycarpa*	*A. taxiformis*
C14:0	3.45 ± 0.54	4.04 ± 0.34	4.03 ± 0.17	4.43 ± 0.83	3.44 ± 0.62	3.74 ± 0.62
iso-C15:0	0.36 ± 0.06	0.34 ± 0.10	0.09 ± 0.02	0.14 ± 0.02	0.23 ± 0.07	0.60 ± 0.09
anteiso-C15:0	0.14 ± 0.04	0.29 ± 0.09	0.02 ± 0.00	0.04 ± 0.01	0.09 ± 0.02	0.17 ± 0.02
C15:0	1.14 ± 0.15	0.34 ± 0.06	0.41 ± 0.07	0.15 ± 0.03	0.73 ± 0.23	1.23 ± 0.21
iso-C16:0	0.23 ± 0.06	0.59 ± 0.18	0.01 ± 0.00	0.15 ± 0.02	0.06 ± 0.02	0.27 ± 0.08
C16:0	40.87 ± 3.97	50.79 ± 0.89	47.15 ± 4.67	47.23 ± 2.45	47.47 ± 1.47	44.63 ± 6.95
C16:1ω9	0.12 ± 0.03	0.06 ± 0.02	0.18 ± 0.05	0.05 ± 0.01	0.18 ± 0.03	0.06 ± 0.01
C16:1ω7	0.66 ± 0.09	0.30 ± 0.06	0.28 ± 0.07	0.18 ± 0.05	0.67 ± 0.13	0.43 ± 0.02
C16:1ω5	0.07 ± 0.02	0.05 ± 0.02	0.03 ± 0.00	0.04 ± 0.01	0.03 ± 0.00	0.14 ± 0.05
C16:2ω6	0.05 ± 0.02	0.01 ± 0.00	0.03 ± 0.00	0.08 ± 0.02	0.08 ± 0.01	0.26 ± 0.08
iso-C17:0	0.12 ± 0.04	0.04 ± 0.01	0.06 ± 0.01	0.02 ± 0.01	0.14 ± 0.04	0.43 ± 0.08
C16:2ω4	0.07 ± 0.02	0.01 ± 0.00	0.07 ± 0.02	0.10 ± 0.03	0.12 ± 0.01	0.18 ± 0.01
anteiso-C17:0	0.13 ± 0.04	0.03 ± 0.01	0.16 ± 0.02	0.11 ± 0.03	0.08 ± 0.02	0.19 ± 0.01
C17:0	0.72 ± 0.14	0.18 ± 0.04	0.16 ± 0.03	0.13 ± 0.03	0.64 ± 0.12	0.94 ± 0.13
C18:1ω12	0.08 ± 0.01	0.05 ± 0.01	0.06 ± 0.01	0.08 ± 0.01	0.10 ± 0.03	0.24 ± 0.03
C18:0	14.35 ± 1.47	31.32 ± 5.14	31.89 ± 3.75	23.67 ± 3.11	18.14 ± 3.29	10.80 ± 0.33
C18:1ω9	1.55 ± 0.23	0.53 ± 0.04	0.49 ± 0.03	1.20 ± 0.21	1.66 ± 0.26	1.54 ± 0.25
C18:1ω7	0.96 ± 0.17	0.18 ± 0.02	0.19 ± 0.05	0.17 ± 0.05	0.66 ± 0.10	2.09 ± 0.43
C18:2ω6	0.40 ± 0.06	0.14 ± 0.02	0.15 ± 0.03	0.12 ± 0.03	0.10 ± 0.02	0.97 ± 0.10
C18:3ω3	0.34 ± 0.04	0.31 ± 0.03	0.24 ± 0.04	0.11 ± 0.02	0.90 ± 0.17	0.71 ± 0.02
C18:4ω3	0.32 ± 0.06	0.18 ± 0.03	0.19 ± 0.02	0.09 ± 0.03	0.54 ± 0.08	0.29 ± 0.03
C20:1ω12	10.18 ± 1.33	1.58 ± 0.17	5.47 ± 0.65	8.21 ± 1.50	9.52 ± 0.93	8.05 ± 1.23
C20:0	0.52 ± 0.08	0.14 ± 0.03	0.49 ± 0.15	0.07 ± 0.02	0.23 ± 0.06	0.37 ± 0.06
C20:1ω11	1.52 ± 0.15	1.19 ± 0.22	1.06 ± 0.16	1.36 ± 0.22	2.26 ± 0.32	1.53 ± 0.20
C20:2ω9	1.91 ± 0.25	0.86 ± 0.07	1.47 ± 0.22	1.15 ± 0.08	1.87 ± 0.28	3.55 ± 0.48
C20:2ω6	0.53 ± 0.08	0.28 ± 0.02	0.13 ± 0.03	0.10 ± 0.01	0.23 ± 0.06	0.91 ± 0.05
C20:4ω6	11.61 ± 1.46	3.13 ± 0.44	3.48 ± 0.24	5.51 ± 0.82	6.81 ± 1.32	5.22 ± 0.66
C20:3ω3	0.29 ± 0.08	0.16 ± 0.05	0.04 ± 0.00	0.10 ± 0.03	0.12 ± 0.03	0.26 ± 0.02
C20:5ω3	5.74 ± 0.97	1.62 ± 0.30	1.27 ± 0.08	4.73 ± 0.92	1.58 ± 0.26	6.05 ± 0.65
C22:1ω7	0.49 ± 0.09	0.10 ± 0.02	0.19 ± 0.01	0.04 ± 0.01	0.34 ± 0.05	0.51 ± 0.08
C22:4ω6	0.34 ± 0.05	0.05 ± 0.01	0.07 ± 0.02	0.04 ± 0.02	0.04 ± 0.01	0.34 ± 0.05
C22:6ω3	0.73 ± 0.21	1.09 ± 0.30	0.43 ± 0.12	0.38 ± 0.07	0.93 ± 0.24	3.31 ± 0.24
TOTAL	100.00	100.00	100.00	100.00	100.00	100.00

relative concentration, was applied. A total of nine compounds (the most abundant FAMEs previously described) were analyzed separately to check for difference among coelomic fluid samples untreated and treated with algae extracts. Minor components were not included in the statistical treatment as their low levels (< 1.0%). The heat map representing the fold changes of FAs registered in the samples analyzed are illustrated in Fig. 2. Statistical analysis revealed a significant ($p < 0.05$) decrease at 24 h of the PUFA and MUFA components as highly susceptible to oxidation mechanisms. On the other hand, SFA concentrations were significantly increased as poorly prone to structure modifications. In detail, at 24 h post-exposure to both extracts, a marked reduction was observed for several FAs in the coelomic fluid of *A. lixula*, such as C18:1ω9, C20:1ω12, C20:1ω11, C20:2ω9, C20:4ω6, and C20:5ω3, all of which showed lower levels compared to the control. However, the statistical analysis highlighted the significant impact of secondary metabolites coming from the *A. taxiformis* genus (invasive Mediterranean species) with respect to the *E. brachycarpa* algal species (endemic Mediterranean species) on the contents of C20:1ω12 (3.45-fold),

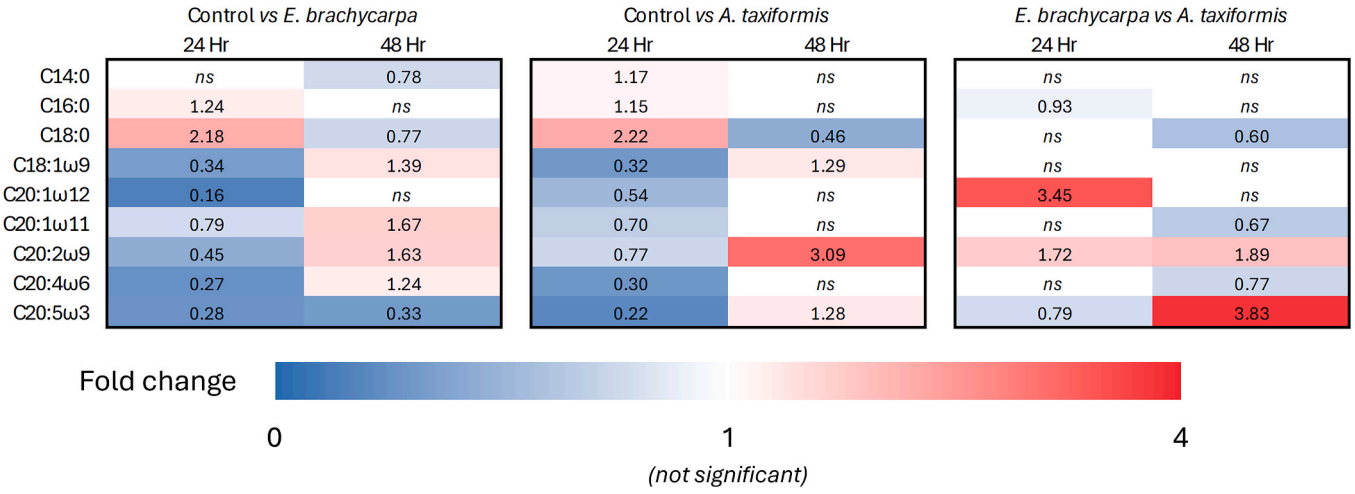

Fig. 2. Heat map of main FAs in celomatic fluids treated with *E. brachycarpa* and *A. taxiformis* extracts after 24 and 48 h. Colors tending to red represent a higher fold change while a lower fold change is depicted by blue color. (For interpretation of the references to color in this figure legend, the reader is referred to the web version of this article.)

C20:2ω9 (1.72-fold), and C20:5ω3 (0.79-fold). In contrast, the content of major fatty acids after 48 h of exposure to secondary metabolites of *E. brachycarpa* tended to increase for most PUFA compounds, surprisingly except for C20:5ω3 (0.33-fold). Indeed, *A. taxiformis* 48 h-treatment showed a neat increase in term of concentration levels only for C20:2ω9 and C20:5ω3 as pictured in Fig. 2 (*E. brachycarpa vs A. taxiformis* at 48 h).

3.2. OPA-amino acids profiling

The HPLC-FLD determination of the total AAs amount in coelomic fluids of *A. lixula* was performed by conversion of the target compounds in OPA-AA derivatives. The on-line derivatization resulted particularly rapid and simple considering that the formation of the OPA-AA derivatives was quantitatively complete in only 7 min at room temp (25 °C). For a global evaluation of the derivatization efficiency, 3 min, 5 min, and 9 min reaction times were also investigated. However, 3 min and 5 min were still not sufficient for the complete recovery of the fifteen OPA-AAs, while 9 min reaction time revealed a decrease in the peak area than 7 min (Fig. S2), probably due to the rapid degradation of the OPA-AA compounds at room temperature. Similar results were also described by Dai et al. (Dai et al., 2014). Consequently, a fully automated on-line pre-column derivatization protocol was developed by using a robotic autosampler system able to prepare and to inject into the HPLC column the OPA-AA compounds.

The HPLC-FLD separative method was optimized and validated for the complete resolution and quantification of the OPA-AA derivatives in the coelomic fluid samples. The HPLC-FLD chromatogram of the AA standards mix containing fifteen AAs and α-aminobutyric acid (ISTD) was illustrated in Fig. S3. Table S2 shows the retention time, linearity range, linear regression equation, coefficients of determination (R^2), LoD and LoQ values obtained for each AA present in the certified standard mixture. All calibration curves were characterized by a satisfactory linearity with R^2 values ≥0.9959. The LoDs and LoQs were calculated as described in the experimental section. The LoDs ranged from a min value of 0.21 (Ser) nmol mL^{-1} to 1.62 (Tyr) nmol mL^{-1}, while the LoQs were between 0.51 (Ser) nmol mL^{-1} and 5.41 (Tyr) nmol mL^{-1}. Therefore, the developed procedure was suitable for quantitative determinations, considering that AAs concentrations in the coelomic fluid samples were significantly above the LoD and LoQ values.

AAs variations in the coelomic fluid samples of *A. lixula*, in response to exposure to secondary metabolites from *A. taxiformis* and *E. brachycarpa* extract of macroalgae were evaluated at 24 h and 48 h. The amounts of AAs are summarized in Table 2. A representative HPLC-FLD chromatogram of OPA-AA derivatives (control sample at 48 h) is illustrated in Fig. 3. An unlabeled peak is present in the HPLC-FLD chromatogram of OPA-AAs in *Arbacia lixula* coelomic fluids at approximately 16 min of elution time. Its identity did not correspond to any of the targeted analytes investigated in the present research. Probably, the unknown compound contains a primary amine that is able to react with the OPA derivatizing agent and therefore can be revealed by the FLD detector. Nevertheless, the peak of the unknown substance is well separated by the others and does not affect the quantification of the target analytes.

The data presented in Table 2 highlight notable differences in the total AAs content expressed in terms of nmol mL^{-1}, while Fig. 4 shows a heat map of the AAs fold changes. Specifically, 24 h after exposure to secondary metabolites from *E. brachycarpa* extract, the coelomic fluid of *A. lixula* exhibited a significant upregulation of several AAs, including His (1.41-fold), Gly (1.29-fold), Ala (1.20-fold), Tyr (1.76-fold), Met (1.12-fold), and Lys (1.64-fold). His and Tyr act as radical scavengers; their increase likely reflects an attempt to buffer ROS accumulation. Meanwhile, Gly and Ala, being glucogenic amino acids, may be involved in energy production, and they also serve as precursors for glutathione (GSH); their peak levels may suggest GSH consumption and a subsequent need for its resynthesis.

Conversely, *A. taxiformis* triggered a more heterogeneous response: while essential AAs such as Ile (0.77-fold), Leu (0.80-fold), and Met (0.27-fold) were downregulated, Tyr (1.72-fold) and Lys (1.26-fold) showed an increase. This behaviour is very evident when comparing directly the effect of secondary metabolites coming from the *A. taxiformis* genus with respect to the *E. brachycarpa* algal species. At 48 h the two treatments showed a similar result where almost all the AAs showed a significant increase.

4. Discussion

4.1. Fatty acid metabolism

The exposure of *A. lixula* to secondary metabolites from *E. brachycarpa* and *A. taxiformis* resulted in marked and time-dependent alterations in lipid metabolism, highlighting the sensitivity of fatty acid pathways to algal-derived chemical stress. As shown in Fig. 2, both algal extracts induced a substantial depletion of oxidation-prone MUFAs and PUFAs at 24 h, accompanied by a concomitant increase in SFAs, particularly stearic acid.

This loss of unsaturated fatty acids may be attributable to reactive oxygen species (ROS)-driven peroxidation initiated by the halogenated metabolites released by *A. taxiformis,* a process widely recognized as a primary driver of oxidative membrane damage (Mortensen et al., 2023). Such evidence is consistent with the findings of Neethu et al. (2017), who demonstrated that the chloroform extract of *Asparagopsis taxiformis*

Table 2
AAs concentrations (nmol mL^{-1} ± standard deviation) in the coelomic fluid of *A. lixula* following 24 h and 48 h of exposure to extracts of *E. brachycarpa* and *A. taxiformis* algae as well as the respective controls (no treatment).

AAs	24 h			48 h		
	Control	*E. brachycarpa*	*A. taxiformis*	Control	*E. brachycarpa*	*A. taxiformis*
Asp	154.73 ± 26.3	153.69 ± 23.91	124.85 ± 19.06	101.81 ± 13.95	155.17 ± 29.22	203.44 ± 14.40
Glu	159.75 ± 16.24	148.43 ± 21.04	154.94 ± 22.13	148.96 ± 18.41	211.19 ± 26.60	280.14 ± 29.31
Ser	146.34 ± 23.7	165.44 ± 29.12	117.98 ± 7.95	97.99 ± 15.14	192.93 ± 31.19	223.42 ± 18.21
His	56.18 ± 5.96	79.35 ± 8.58	32.53 ± 5.54	50.95 ± 5.88	55.30 ± 8.59	90.41 ± 11.60
Gly	1259.46 ± 167.87	1620.04 ± 231.99	1401.43 ± 158.46	1594.71 ± 233.17	2187.63 ± 299.76	3299.06 ± 339.57
Arg	105.04 ± 5.78	117.86 ± 19.52	76.78 ± 6.28	79.14 ± 10.63	122.02 ± 19.48	154.38 ± 17.65
Thr	129.29 ± 19.38	148.53 ± 15.31	111.37 ± 17.20	104.06 ± 10.92	141.93 ± 20.38	193.42 ± 20.72
Ala	153.47 ± 26.75	184.55 ± 8.92	125.30 ± 8.58	117.44 ± 8.52	190.18 ± 30.63	235.83 ± 22.00
Tyr	72.46 ± 7.76	127.86 ± 17.64	124.98 ± 17.43	124.36 ± 19.55	119.28 ± 15.73	181.59 ± 25.09
Met	34.84 ± 2.85	38.95 ± 3.26	9.31 ± 0.30	29.88 ± 5.04	32.02 ± 5.65	68.94 ± 8.37
Val	104.61 ± 9.07	110.96 ± 17.93	79.48 ± 10.88	74.51 ± 6.48	113.74 ± 16.21	146.78 ± 16.54
Phe	66.57 ± 10.35	79.34 ± 11.44	55.37 ± 8.78	57.89 ± 6.32	71.52 ± 13.05	108.10 ± 17.12
Ile	68.97 ± 10.45	78.83 ± 11.95	53.06 ± 6.88	60.27 ± 10.05	77.18 ± 12.98	115.21 ± 13.75
Leu	137.06 ± 21.07	151.43 ± 27.45	109.31 ± 14.73	130.82 ± 20.31	161.79 ± 26.06	204.58 ± 20.16
Lys	226.29 ± 41.84	372.22 ± 62.26	286.20 ± 52.04	296.49 ± 47.82	409.86 ± 42.46	534.96 ± 53.75

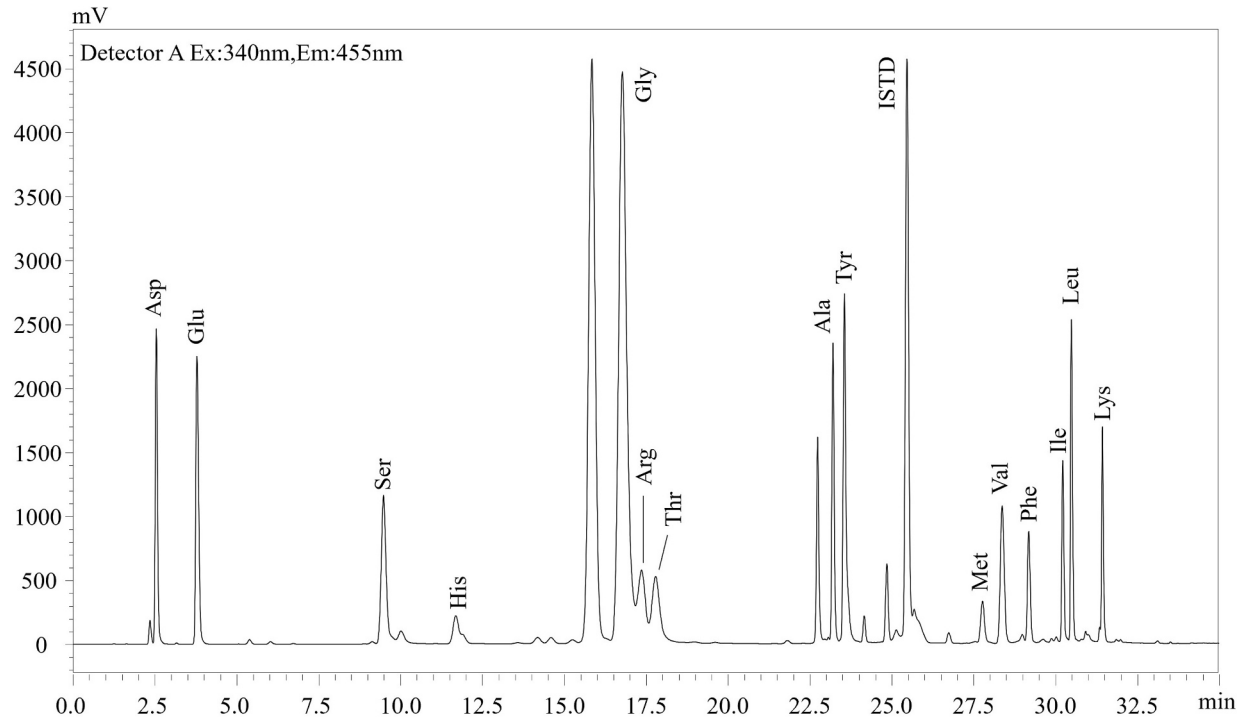

Fig. 3. HPLC-FLD chromatogram of OPA-AAs in *Arbacia lixula* coelomic fluid (control sample at 48 h).

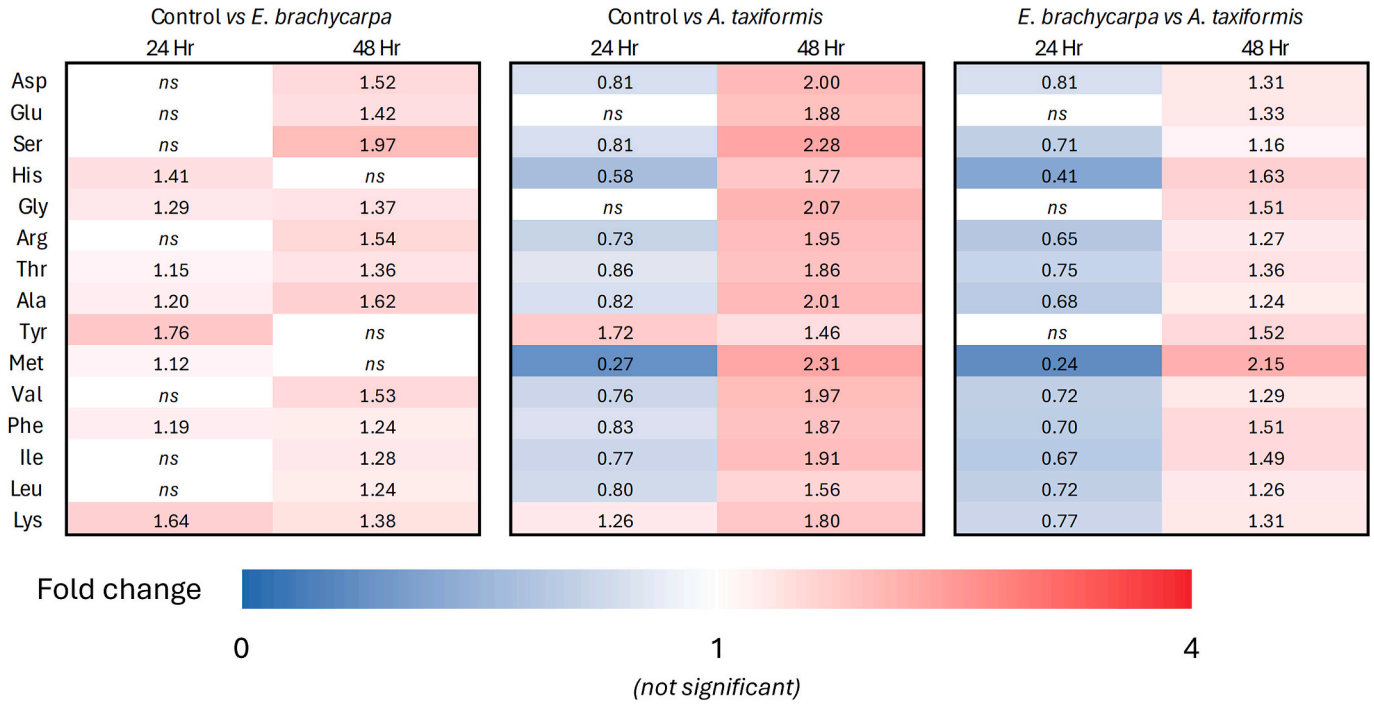

Fig. 4. Heat map of the AAs in celomatic fluids treated with *E. brachycarpa* and *A. taxiformis* extracts after 24 and 48 h. Colors tending to red represent a higher fold change while a lower fold change is depicted by blue color. (For interpretation of the references to color in this figure legend, the reader is referred to the web version of this article.)

contains the highest total flavonoid content among tested fractions. However, antioxidant capacity assessed *in vitro* does not necessarily correspond to a reduced oxidative impact *in vivo*, particularly when highly redox-active flavonoids and halogenated metabolites directly interact with biological membranes. Under these conditions, such compounds may promote transient oxidative pressure, thereby triggering lipid peroxidation and subsequent membrane remodeling. Accordingly, the oxidative stress and lipid reorganization observed in *Arbacia lixula* may be mediated by the high chemical reactivity of *A. taxiformis* secondary metabolites rather than by a purely protective antioxidant effect. In parallel, the marked increase of C18:0 (2.22-fold *vs.* control) points to a transient "hardening" of the lipid bilayer through the selective accumulation or *de novo* synthesis of saturated acids that are less prone to peroxidation. At 48 h, the lipid response diverged

between treatments. In *A. taxiformis*-exposed individuals, the sharp decline of C18:0 was accompanied by a significant recovery of PUFAs, including eicosapentaenoic and eicosadienoic acids. This temporal pattern is consistent with compensatory lipid remodeling processes that may contribute to restoring membrane physical properties and cellular homeostasis following an initial oxidative insult. Indeed, fatty acid profiles in sea urchins have been shown to shift dynamically under oxidative stress, and membrane lipid composition represents a key structural target of reactive species (Fouzai et al., 2023; Naudí et al., 2013).

In contrast, exposure to *E. brachycarpa* resulted in a marked but comparatively less intense depletion of unsaturated fatty acids at 24 h, followed by a partial and selective recovery at 48 h, involving MUFAs such as C18:1ω9, C20:1ω11, and PUFAs, including C20:2ω9, C20:4ω6 together with a concomitant decrease in C18:0. This pattern is consistent with a more controlled redox modulation, likely related to the diterpene-rich chemical profile of *E. brachycarpa*, which appears to exert a milder and less acutely reactive metabolic effect. This slower and less pronounced remodeling suggests a more moderate and potentially transient adaptive response, in which membrane fatty acid composition is dynamically adjusted to counteract oxidative perturbations and preserve cellular homeostasis (Fouzai et al., 2023; Naudí et al., 2013). Importantly, similar physiological and metabolic endpoints have been documented under ecologically realistic exposure scenarios. Feeding experiments and field-based studies have shown that the consumption of both native and invasive macroalgae, including *A. taxiformis*, can induce sublethal responses in sea urchins involving antioxidant defenses, lipid peroxidation, and shifts in energy allocation (Quetglas-Llabrés et al., 2020; Tejada et al., 2013). Although these studies integrate trophic processes absent from the present experimental design, they support the ecological relevance of the metabolic pathways identified here as sensitive targets of algal chemical stress. Nevertheless, an important methodological limitation must be acknowledged: direct exposure was based on direct injection of algal extracts, which differs from the primary natural pathway through which sea urchins encounter algal secondary metabolites, namely ingestion. Injection-based exposure bypasses key trophic processes such as feeding behaviour, digestion, absorption, and metabolic transformation, and may therefore influence the magnitude and temporal dynamics of lipid responses compared to feeding-based approaches. Accordingly, the lipid responses described here should be interpreted as mechanistic indicators of direct physiological sensitivity to algal secondary metabolites rather than as a full proxy for natural trophic interactions. Feeding-based experiments, such as those reported by Pereira et al. (2024), remain essential for integrating ecological realism and should be considered a priority for future studies.

4.2. Amino acid metabolism

In parallel with lipid remodeling, exposure to algal secondary metabolites induced significant and time-dependent alterations in amino acid profiles in coelomic fluids of *A. lixula*. Following 24 h exposure to *E. brachycarpa*, several functionally relevant amino acids including histidine, glycine, alanine, tyrosine, methionine, and lysine were selectively upregulated. Histidine and tyrosine may contribute to ROS buffering (Davies, 2005; Halliwell and Gutteridge, 2015), whereas glycine and alanine are involved in both energy metabolism and glutathione biosynthesis, suggesting an early activation of antioxidant and metabolic defense pathways (Dong et al., 2022).

In contrast, exposure to *A. taxiformis* induced a more heterogeneous amino acid response at 24 h, characterized by the downregulation of essential amino acids such as isoleucine, leucine, and methionine, alongside increased levels of tyrosine and lysine. The reduction of branched-chain amino acids and methionine may reflect a stress-induced reallocation of nitrogen resources aimed at preserving structural proteins and maintaining the availability of S-adenosylmethionine, a key methyl-group donor involved in phospholipid methylation and antioxidant defense pathways (Giannetto et al., 2018).

At 48 h, both algal extracts promoted a generalized increase in amino acid concentrations, with *A. taxiformis* eliciting the most pronounced response. Substantial increases were observed for methionine, glycine, alanine, serine, glutamate, and aspartate, suggesting a delayed hyper-compensatory response potentially associated with recovery processes or sustained metabolic stress. Similar shifts in amino acid metabolism and energy allocation have been reported in feeding and field-based studies on sea urchins exposed to macroalgae, supporting the ecological relevance of the metabolic pathways highlighted here (Quetglas-Llabrés et al., 2020; Tejada et al., 2013). As for lipid metabolism, the interpretation of amino acid responses must consider the absence of compound-specific chemical characterization of the algal extracts and the use of an injection-based exposure approach. Accordingly, the observed modulation of amino acid profiles is discussed as an indicator of general metabolic and redox adjustments in response to algal chemical stress, rather than as a direct representation of ingestion-mediated physiological processes under natural feeding conditions.

5. Conclusion

In this study, we provided a first assessment of how secondary metabolites produced by the macroalgae *E. brachycarpa* and *A. taxiformis* can reshape fatty acids and amino acids homeostasis in the coelomic fluid of the sea urchin *A. lixula*. After 24 h, a clear lipid remodeling was observed. *A. taxiformis* caused a marked depletion of oxidation-prone MUFAs and PUFAs (*e.g.*, C18:1ω9 and C20:5ω3), accompanied by a more than twofold increase in stearic acid, also known for its oxidative stability. These findings indicate an emergency response aimed at stabilizing membranes through the accumulation of more resistant saturated lipids. In contrast, *E. brachycarpa* induced similar but less pronounced changes, indicating a milder oxidative impact. This milder effect may be linked to the nature of its bioactive constituents, particularly diterpenes, which are less reactive than the halogenated metabolites of *A. taxiformis*. At 48 h, partial homeostatic recovery was observed, especially in *A. taxiformis* treated samples, where the previously elevated C18:0 levels decreased sharply (0.46-fold), while peroxidation-sensitive PUFAs such as C20:5ω3 and C20:2ω9 increased (1.28-fold and 3.09-fold, respectively). This reversal supports the interpretation of C18:0 accumulation as a transient defensive adaptation, followed by membrane repair and functional lipid restoration. At the same time, *E. brachycarpa* exposure led to a more progressive increase in unsaturated FAs such as C20:1ω11, C20:2ω9, and C20:4ω6, consistent with a slow, controlled remodeling strategy. The different lipid responses appear closely linked to the distinct ecological and chemical nature of the algal metabolites. *A. taxiformis*, as an invasive species, releases highly oxidizing compounds, especially polyhalomethanes catalyzed by haloperoxidases (*e.g.*, $CHCl_3$, CH_2Br_2), which can trigger acute damage followed by a fast “repair-and-replace” cellular response (McConnell and Fenical, 1977; Neumann et al., 2008). In contrast, the endemic *E. brachycarpa* appears to induce a milder and more controlled metabolic adaptation. These dynamics are in line with findings from Pereira et al. (2024), who showed that *A. taxiformis*, when included in the diet of *Diplodus sargus* under simulated marine heatwave conditions, stimulated antioxidant enzyme activity (CAT, GST) and energy metabolism (citrate synthase), reducing lipid peroxidation. This biphasic pattern, initial damage followed by adaptive response, supports the idea that halogenated metabolites may function as oxidative stressors that induce compensatory metabolism. In contrast, *E. brachycarpa* triggered more moderate and progressive lipid changes, consistent with a controlled remodeling strategy and a lower oxidative impact, likely reflecting differences in the reactivity of its secondary metabolites. Amino acid dynamics further revealed species-specific metabolic strategies. While *E. brachycarpa* promoted an early, targeted mobilization of functionally relevant amino acids linked to antioxidant

defense and energy metabolism, *A. taxiformis* induced a delayed but marked hypercompensatory response, suggesting intensified redox regulation and metabolic reprogramming following initial stress.

Although the present experimental design does not replicate the natural trophic exposure of sea urchins to algal secondary metabolites through ingestion, the use of intracoelomic injection provided a controlled framework to isolate the direct physiological effects of algal-derived compounds. By minimizing variability associated with feeding behaviour, digestion, and bioavailability, this approach allowed the detection of rapid and sublethal metabolic responses. Future studies integrating feeding-based experiments with detailed chemical characterization of algal metabolites will be essential to fully assess the ecological relevance of these responses under natural conditions.

CRediT authorship contribution statement

Manuela Mauro: Writing – review & editing, Supervision, Methodology. **Rosario Badalamenti:** Supervision, Methodology. **Giovanna Cafeo:** Writing – original draft, Visualization, Formal analysis, Data curation. **Valentina Chiaia:** Writing – original draft, Validation, Formal analysis, Data curation. **Danilo Donnarumma:** Writing – original draft, Validation, Methodology, Data curation. **Mirella Vazzana:** Writing – review & editing, Supervision, Methodology. **Vincenzo Arizza:** Writing – review & editing, Supervision, Resources, Methodology. **Giuseppe Micalizzi:** Writing – review & editing, Writing – original draft, Supervision, Methodology, Data curation. **Paola Dugo:** Writing – review & editing, Supervision, Methodology. **Luigi Mondello:** Writing – review & editing, Supervision, Resources. **Francesca Falco:** Writing – review & editing, Writing – original draft, Supervision, Conceptualization.

Declaration of competing interest

The authors declare that they have no known competing financial interests or personal relationships that could have appeared to influence the work reported in this paper.

Acknowledgements

The authors acknowledge Merck Life Science and Shimadzu Corporations for their continuous support.

Appendix A. Supplementary data

Supplementary data to this article can be found online at https://doi.org/10.1016/j.jembe.2026.152169.

Data availability

Data will be made available on request.

References

Agnetta, D., Badalamenti, F., Ceccherelli, G., Di Trapani, F., Bonaviri, C., Gianguzza, P., 2015. Role of two co-occurring Mediterranean Sea urchins in the formation of barren from *Cystoseira* canopy. Estuar. Coast. Shelf Sci. 152, 73–77. https://doi.org/10.1016/j.ecss.2014.11.023.

Amico, V., Oriente, G., Piattelli, M., Ruberto, G., Tringali, C., 1981. Novel acyclic diterpenes from the brown alga *Cystoseira crinita*. Phytochemistry 20, 1085–1088. https://doi.org/10.1016/0031-9422(81)83032-4.

Ballesteros, E., Rodríguez-Prieto, C., 1996. Presència d'A. taxiformis (Delile) Trevisan a Balears. Boll. Soc. Hist. Nat. Balears. 39, 135–138.

Ballesteros, E., Garrabou, J., Hereu, B., Zabala, M., Cebrian, E., Sala, E., 2009. Deep-water stands of *Cystoseira zosteroides* C. Agardh (Fucales, Ochrophyta) in the northwestern Mediterranean: insights into assemblage structure and population dynamics. Estuar. Coast. Shelf Sci. 82, 477–484. https://doi.org/10.1016/j.ecss.2009.02.013.

Barone, R., Mannino, A.M., Marino, M., 2003. *A. taxiformis* (Bonnemaisoniales, Rhodophyta): first record of gametophytes on the Italian coast. Bocconea 16, 1021–1025.

Beijnink, F.B., Van Der Sluis, I., Voogt, P.A., 1984. Turnover rates of fatty acid and amino acid in the coelomic fluid of the sea star Asterias rubens: implications for the route of nutrient translocation during vitellogenesis. Compar. Biochem. Physiol. Part B, Biochem. Mol. Biol. 78, 761–767. https://doi.org/10.1016/0305-0491(84)90131-7.

Bligh, E.G., Dyer, W.J., 1959. A rapid method of total lipid extraction and purification. Can. J. Biochem. Physiol. 37, 911–917. https://doi.org/10.1139/o59-099.

Bonaviri, C., Vega Fernández, T., Fanelli, G., Badalamenti, F., Gianguzza, P., 2011. Leading role of the sea urchin *Arbacia lixula* in maintaining the barren state in southwestern Mediterranean. Mar. Biol. 158, 2505–2513. https://doi.org/10.1007/s00227-011-1751-2.

Budzałek, G., Śliwińska-Wilczewska, S., Wiśniewska, K., Wochna, A., Bubak, I., Latała, A., Wiktor, J.M., 2021. Macroalgal defense against competitors and herbivores. Int. J. Mol. Sci. 22, 7865. https://doi.org/10.3390/ijms22157865.

Butler, A., Carter-Franklin, J.N., 2004. The role of vanadium bromoperoxidase in the biosynthesis of halogenated marine natural products. Nat. Prod. Rep. 21, 180. https://doi.org/10.1039/b302337k.

Butler, A., Sandy, M., 2009. Mechanistic considerations of halogenating enzymes. Nature 460, 848–854. https://doi.org/10.1038/nature08303.

Cheminée, A., Sala, E., Pastor, J., Bodilis, P., Thiriet, P., Mangialajo, L., Cottalorda, J.-M., Francour, P., 2013. Nursery value of Cystoseira forests for Mediterranean rocky reef fishes. J. Exp. Mar. Biol. Ecol. 442, 70–79. https://doi.org/10.1016/j.jembe.2013.02.003.

Dai, Z., Wu, Z., Jia, S., Wu, G., 2014. Analysis of amino acid composition in proteins of animal tissues and foods as pre-column o-phthaldialdehyde derivatives by HPLC with fluorescence detection. J. Chromatogr. B 964, 116–127. https://doi.org/10.1016/j.jchromb.2014.03.025.

Davies, M.J., 2005. The oxidative environment and protein damage. Biochim. Biophys. Acta, Proteins Proteomics 1703, 93–109. https://doi.org/10.1016/j.bbapap.2004.08.007.

Directive 2000/60/EC, 2000. Directive 2000/60/EC of the European Parliament and of the Council of 23 October 2000 establishing a framework for Community action in the field of water policy.

Dong, X., Yang, Z., Liu, Z., Wang, X., Yu, H., Peng, C., Hou, X., Lu, W., Xing, Q., Hu, J., Huang, X., Bao, Z., 2022. Metabonomic analysis provides new insights into the response of Zhikong scallop (*Chlamys farreri*) to heat stress by improving energy metabolism and antioxidant capacity. Antioxidants 11, 1084. https://doi.org/10.3390/antiox11061084.

El-Beltagi, H.S., Mohamed, A.A., Mohamed, H.I., Ramadan, K.M.A., Barqawi, A.A., Mansour, A.T., 2022. Phytochemical and potential properties of seaweeds and their recent applications: a review. Marine Drugs 20, 342. https://doi.org/10.3390/md20060342.

El-Sheekh, M., Fathy, A.A., Saber, H., Saber, A.A., 2022. Medicinal and pharmaceutical applications of seaweeds. Egypt. J. Bot. 63, 1–29. https://doi.org/10.21608/ejbo.2022.145631.2022.

Eurachem Guide, 2025. Eurachem Guide: the fitness for purpose of analytical methods – A laboratory Guide to method validation and related topics, (3rd ed. 2025).

Fouzai, C., Trabelsi, W., Bejaoui, S., Marengo, M., Ghribi, F., Chetoui, I., Mili, S., Soudani, N., 2023. Dual oxidative stress and fatty acid profile impacts in *Paracentrotus lividus* exposed to lambda-cyhalothrin: biochemical and histopathological responses. Toxicol. Res. 39, 429–441. https://doi.org/10.1007/s43188-023-00174-4.

Giannetto, A., Cappello, T., Oliva, S., Parrino, V., De Marco, G., Fasulo, S., Mauceri, A., Maisano, M., 2018. Copper oxide nanoparticles induce the transcriptional modulation of oxidative stress-related genes in *Arbacia lixula* embryos. Aquat. Toxicol. 201, 187–197. https://doi.org/10.1016/j.aquatox.2018.06.010.

Halliwell, B., Gutteridge, J.M.C., 2015. Free radicals in biology and medicine. Oxford University Press. https://doi.org/10.1093/acprof:oso/9780198717478.001.0001.

Hay, M.E., 2009. Marine chemical ecology: chemical signals and cues structure marine populations, communities, and ecosystems. Annu. Rev. Mar. Sci. 1, 193–212. https://doi.org/10.1146/annurev.marine.010908.163708.

Liyana-Pathirana, C., Shahidi, F., Whittick, A., 2002. Comparison of nutrient composition of gonads and coelomic fluid of green sea urchin *Strongylocentrotus droebachiensis*. J. Shellfish Res. 21, 861–870.

Mancuso, F.P., D'Agostaro, R., Milazzo, M., Badalamenti, F., Musco, L., Mikac, B., Lo Brutto, S., Chemello, R., 2022. The invasive seaweed *Asparagopsis taxiformis* erodes the habitat structure and biodiversity of native algal forests in the Mediterranean Sea. Mar. Environ. Res. 173, 105515. https://doi.org/10.1016/j.marenvres.2021.105515.

Maschek, J.A., Baker, B.J., 2008. The chemistry of algal secondary metabolism. In: Amsler, C.D. (Ed.), Algal Chemical Ecology. Springer, Berlin Heidelberg, Berlin, Heidelberg, pp. 1–24. https://doi.org/10.1007/978-3-540-74181-7_1.

Matos, G.S., Pereira, S.G., Genisheva, Z.A., Gomes, A.M., Teixeira, J.A., Rocha, C.M.R., 2021. Advances in extraction methods to recover added-value compounds from seaweeds: sustainability and functionality. Foods 10, 516. https://doi.org/10.3390/foods10030516.

McConnell, O., Fenical, W., 1977. Halogen chemistry of the red alga *Asparagopsis*. Phytochemistry 16, 367–374. https://doi.org/10.1016/0031-9422(77)80067-8.

Micalizzi, G., Chiaia, V., Mancuso, M., Bottari, T., Mghili, B., D'Angelo, G., Falco, F., Mondello, L., 2024. Investigating the effects of microplastics on the metabolism of *Trematomus bernacchii* from the ross sea (Antarctica). Sci. Total Environ. 955, 176766. https://doi.org/10.1016/j.scitotenv.2024.176766.

Mishra, A.K., 2018. Sargassum, Gracilaria and Ulva exhibit positive antimicrobial activity against human pathogens. OALib 05, 1–11. https://doi.org/10.4236/oalib.1104258.

Mortensen, M.S., Ruiz, J., Watts, J.L., 2023. Polyunsaturated fatty acids drive lipid peroxidation during Ferroptosis. Cells 12, 804. https://doi.org/10.3390/cells12050804.

Naudí, A., Jové, M., Ayala, V., Portero-Otín, M., Barja, G., Pamplona, R., 2013. Membrane lipid unsaturation as physiological adaptation to animal longevity. Front. Physiol. 4. https://doi.org/10.3389/fphys.2013.00372.

Neethu, P., Suthindhiran, K., Jayasri, M., 2017. Antioxidant and antiproliferative activity of *Asparagopsis Taxiformis*. Pharm. Res. 9, 238. https://doi.org/10.4103/pr.pr_128_16.

Neumann, C.S., Fujimori, D.G., Walsh, C.T., 2008. Halogenation strategies in natural product biosynthesis. Chem. Biol. 15, 99–109. https://doi.org/10.1016/j.chembiol.2008.01.006.

Nunes, N., Valente, S., Ferraz, S., Barreto, M.C., Pinheiro De Carvalho, M.A.A., 2018. Nutraceutical potential of *Asparagopsis taxiformis* (Delile) Trevisan extracts and assessment of a downstream purification strategy. Heliyon 4, e00957. https://doi.org/10.1016/j.heliyon.2018.e00957.

Paul, C., Pohnert, G., 2011. Production and role of volatile halogenated compounds from marine algae. Nat. Prod. Rep. 28, 186–195. https://doi.org/10.1039/C0NP00043D.

Pereira, A., Marmelo, I., Dias, M., Silva, A.C., Grade, A.C., Barata, M., Pousão-Ferreira, P., Dias, J., Anacleto, P., Marques, A., Diniz, M.S., Maulvault, A.L., 2024. *Asparagopsis taxiformis* as a novel antioxidant ingredient for climate-smart aquaculture: antioxidant, metabolic and digestive modulation in juvenile white seabream (*Diplodus sargus*) exposed to a marine heatwave. Antioxidants 13, 949. https://doi.org/10.3390/antiox13080949.

Pereira, D.M., Valentão, P., Teixeira, N., Andrade, P.B., 2013. Amino acids, fatty acids and sterols profile of some marine organisms from Portuguese waters. Food Chem. 141, 2412–2417. https://doi.org/10.1016/j.foodchem.2013.04.120.

Piazzi, L., Ceccherelli, G., 2019. Effect of sea urchin human harvest in promoting canopy forming algae restoration. Estuar. Coast. Shelf Sci. 219, 273–277. https://doi.org/10.1016/j.ecss.2019.02.028.

Ponte, J.M.S., Seca, A.M.L., Barreto, M.C., 2022. *Asparagopsis genus*: what we really know about its biological activities and chemical composition. Molecules 27, 1787. https://doi.org/10.3390/molecules27061787.

Privitera, D., Chiantore, M., Mangialajo, L., Glavic, N., Kozul, W., Cattaneo-Vietti, R., 2008. Inter- and intra-specific competition between *Paracentrotus lividus* and *Arbacia lixula* in resource-limited barren areas. J. Sea Res. 60, 184–192. https://doi.org/10.1016/j.seares.2008.07.001.

Quetglas-Llabrés, M.M., Tejada, S., Capó, X., Langley, E., Sureda, A., Box, A., 2020. Antioxidant response of the sea urchin *Paracentrotus lividus* to pollution and the invasive algae *Lophocladia lallemandii*. Chemosphere 261, 127773. https://doi.org/10.1016/j.chemosphere.2020.127773.

Shalaby, E.A., Shanab, S.M.M., 2021. Antiviral activity of extract and purified compound from red macroalgae *Asparagopsis taxiformis* against H5N1 virus. Univ. J. Pharm. Res. https://doi.org/10.22270/ujpr.v6i2.573.

Tejada, S., Deudero, S., Box, A., Sureda, A., 2013. Physiological response of the sea urchin *Paracentrotus lividus* fed with the seagrass *Posidonia oceanica* and the alien algae *Caulerpa racemosa* and *Lophocladia lallemandii*. Mar. Environ. Res. 83, 48–53. https://doi.org/10.1016/j.marenvres.2012.10.008.

Terwilliger, D.P., Buckley, K.M., Brockton, V., Ritter, N.J., Smith, L.C., 2007. Distinctive expression patterns of 185/333 genes in the purple sea urchin, *Strongylocentrotus purpuratus*: an unexpectedly diverse family of transcripts in response to LPS, β-1,3-glucan, and dsRNA. BMC Mol. Biol. 8, 16. https://doi.org/10.1186/1471-2199-8-16.

Thépot, V., Campbell, A.H., Rimmer, M.A., Jelocnik, M., Johnston, C., Evans, B., Paul, N. A., 2022. Dietary inclusion of the red seaweed *Asparagopsis taxiformis* boosts production, stimulates immune response and modulates gut microbiota in Atlantic salmon, *Salmo salar*. Aquaculture 546, 737286. https://doi.org/10.1016/j.aquaculture.2021.737286.

Tsiamis, K., Panayotidis, P., 2007. First record of the red alga *Asparagopsis taxiformis* (Delile) Trevisan de saint-Léon in Greece. AI 2, 435–438. https://doi.org/10.3391/ai.2007.2.4.14.

Zanolla, M., Carmona, R., De La Rosa, J., Altamirano, M., 2018. Structure and temporal dynamics of a seaweed assemblage dominated by the invasive lineage 2 of *Asparagopsis taxiformis* (Bonnemaisoniaceae, Rhodophyta) in the Alboran Sea. Mediterr. Mar. Sci. 19, 147. https://doi.org/10.12681/mms.1892.